Review

Biological Psychiatry

Ultrasonic Neuromodulation for Network Treatments of Psychiatric and Neurological Disorders

Jan Kubanek

ABSTRACT

Transcranial focused ultrasound provides the missing tool for modulation and reset of deep neural circuits. The noninvasiveness, flexibility, and spatial precision of the tool open new opportunities for causal interrogation of brain function and for personalized diagnoses and treatments of mental and neurological disorders. This article reviews the current state of the art in regard to emerging clinical applications to affective disorders, chronic pain, disorders of consciousness, and thought-related disorders. The article provides practical guidelines for applying this powerful tool to patients in a safe, controlled, and reproducible manner. The guidelines include the identification of appropriate treatment targets, compensation for the ultrasound attenuation by the skull and head, targeting and dosing validation, selection of effective and safe stimulation parameters, and considerations for inducing sustained therapeutic effects.

https://doi.org/10.1016/j.biopsych.2026.01.010

ULTRASONIC NEUROMODULATION

Purpose and Strengths

Psychiatric and neurological disorders affect nearly one-fourth of the world's population (1,2). On average, an estimated one-third of patients are resistant to current treatments (3–13). Treatments that could directly target the involved neural circuits are complicated by the fact that psychiatric and neurological disorders involve neural networks situated deep in the brain, including limbic, basal ganglia, thalamic, and brain stem networks (14–20). Neuromodulation has the potential to provide a targeted reset of these circuits (21–23), but current approaches either require surgeries (24,25) or do not reach the necessary intensity and focus at depth (26–28).

Transcranial focused ultrasound combines noninvasiveness and focus at depth (Figure 1A). This is possible due to sound propagating through biological tissues much more slowly (about 1 mile/s) than electromagnetic waves (about 186,000 miles/s). The relatively slow propagation speed offers a favorably small wavelength—on the order of 2 to 5 mm—for frequencies that effectively penetrate the skull (29–31). This has two key benefits: First, due to diffraction, the ultrasound can be focused into an area of approximately that order (Figure 1). Second, as a wave, ultrasound provides high intensity at the target (constructive interference) and low intensity at the source, as desired in most clinical applications. These strengths position focused ultrasound as the missing tool to modulate deep brain circuits in humans noninvasively and selectively.

Effectiveness

When applied to rodent motor cortex under appropriate anesthesia (32), ultrasound evokes overt motor responses (32–36). Low-intensity ultrasound can also trigger changes in motor behavior in humans, when accounting for the distortions of ultrasound by the human skull and air cavities between the hair and acoustic coupling (see Accounting for Skull and Hair). For example, just seconds of controlled modulation of the ventral intermediate nucleus of the thalamus can substantially suppress essential tremor (Figure 1B). These neurosuppressive effects have been observed by multiple groups (37–40). The suppressive effects can also be observed on functional magnetic resonance imaging (fMRI) scans (Figure 1A), specifically at the ultrasound target (41–45). In addition, when aberrations by the skull are taken into account, ultrasound can provide notable sensations, evoking phosphenes (46) or activating nerves (47).

Applicable Mechanisms

Ultrasonic neuromodulation involves 4 classes of primary mechanisms, engagement of which is parameter dependent (Figure 2). For applications through the human skull, which harness a favorable transmission window in the 0.2- to 0.8-MHz frequency range (29–31,48), 2 classes are preferentially at play.

First, the time-varying pressure wave of peak pressure amplitude P_m and the associated average intensity $I = \frac{P_m^2}{2Z}$ periodically displaces particles, molecules, and membranes. The maximal displacement of a particle or molecule occurs over half of the period: $\xi_m = \frac{P_m}{Z}\int_0^{T/2}\sin(2\pi ft)dt = \frac{P_m}{Z\pi f} = \frac{\sqrt{2I}Z}{Z\pi f}$, where Z is the acoustic impedance of the medium. With typical neuromodulation parameters, the maximum displacement of molecules in water (acoustic impedance $Z \approx 1.5$ MRayl) reaches about 0.1 to 1 μm. Such displacements may be sufficient to periodically activate mechanoreceptors and

ISSN: 0006-3223

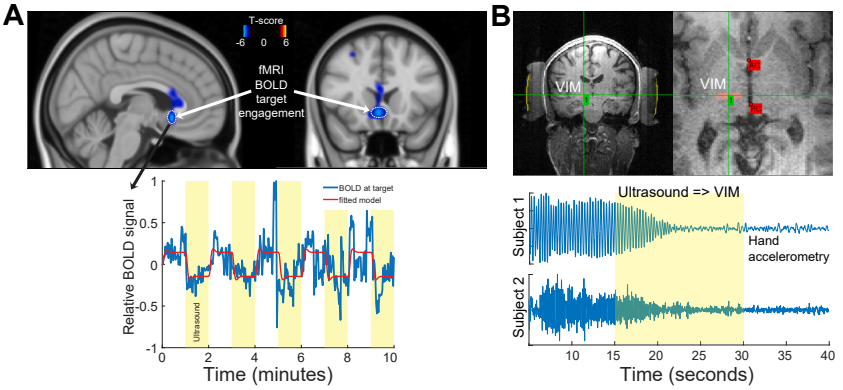

Figure 1. Strengths of ultrasonic neuromodulation. **(A)** Selective engagement of confined targets deep in the brain. (Top) One-minute epochs of ultrasound, interleaved with 1-minute epochs of no ultrasound, modulate magnetic resonance imaging (MRI) blood oxygen level–dependent (BOLD) signals (1 participant) specifically at the target, the subcallosal cingulate cortex. The procedure is detailed in a recent study (44). (Bottom) Example BOLD signal modulation. **(B)** Modulation of motor behavior in humans. Example modulation of the ventral intermediate nucleus (VIM) of the thalamus with inhibitory pulses (37), leading to rapid suppression of essential tremor. AC, anterior commissure; fMRI, functional MRI; PC, posterior commissure.

ion channels (49–61). Moreover, it has been suggested that high-frequency ultrasound vibrations may trigger membrane oscillations that are slow enough to produce spiking activity due to concomitant changes in membrane capacitance (62). In both cases, these mechanical effects increase with the ultrasound intensity *I* and are inversely proportional to frequency *f* (see the effect arrow in Figure 2).

Second, the displacement may be enhanced by the formation of gas nuclei in the tissue, a phenomenon referred to as cavitation. Cavitation nuclei oscillate at the fundamental frequency of the ultrasound and cause displacements much greater than the inherent particle displacement (63) while stable and safe. One particular type of stable cavitation that may be involved in ultrasonic neuromodulation is intramembrane cavitation (64–66). In this mechanism, air cavities form and oscillate within leaflets of membranes, leading to periodic changes in membrane capacitance. These oscillations, when rectified by ion channels, may lead to integration of membrane potential over time and the generation of action potentials (65). The likelihood of cavitation increases with ultrasound intensity *I* and decreases with its frequency *f* and is often approximated using mechanical index (MI)–related metrics in the form of $MI = \frac{P_m}{\sqrt{f}} = \sqrt{\frac{2IZ}{f}}$ (67).

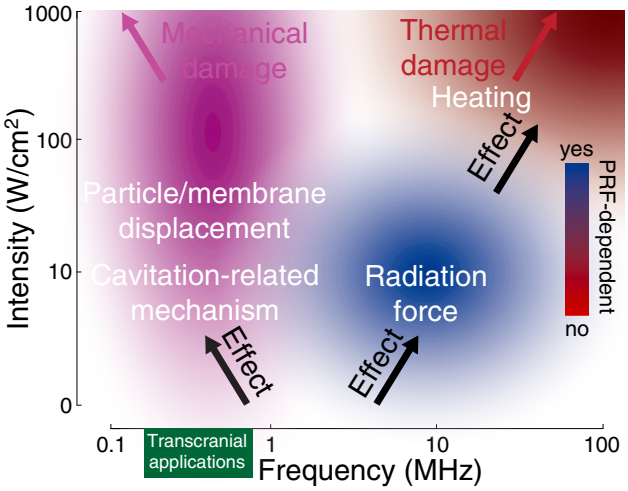

Figure 2. Primary mechanisms involved in ultrasonic neuromodulation. The figure shows 4 main classes of mechanisms (white text) as a function of the ultrasound frequency (abscissa) and intensity (ordinate). Within each class, the black arrow with the effect label points in the direction of increasing effect magnitude (see specific equations in the main text). The purple and red arrows indicate regions of high likelihood of mechanical and thermal damage, respectively. The colors and the associated color bar indicate dependence on the ultrasound pulse repetition frequency (PRF). The green bar on the bottom shows the window of frequencies for favorable transmission through the human skull. All mechanisms substantially overlap, including radiation force, which increases in the region of heating (omitted for clarity).

At higher frequencies of the ultrasound, around 2 MHz, the absorption of ultrasound by biological tissues becomes appreciable (68), leading to substantial attenuation α and preferential engagement of the other 2 classes of mechanisms.

First, the attenuation produces intensity gradients that result in radiation forces that can activate ion channels (49–61). The radiation forces push on a target throughout the application of each burst of ultrasound. Thus, the resulting effects on membranes and ion channels depend on the pulse repetition frequency (PRF) (69,70) (see color bar in Figure 2). This is because each membrane-ion channel complex forms a mechanoelectrical transduction system with a specific resonance frequency—the optimal PRF for that ion channel and cell type (51,69,70). The radiation pressure due to attenuation in a plane wave can be approximated as $p_r = \frac{2\alpha I}{c}\Delta z$, where *c* is the speed of sound in the medium and Δz is the elemental distance (e.g., the diameter of a cell) over which the radiation pressure gradient is evaluated. Because α is approximately proportional to *f* in brain tissues ($\alpha \propto f$), the effects of radiation force due to attenuation are proportional to ultrasound frequency (Figure 2).

Second, high absorption can also lead to an appreciable rise in temperature that can also activate ion channels (50,55–57,71). If the rise in temperature is kept within applicable safety levels (72,73), this mechanism could be harnessed for neuromodulation (74,75). Maximal temperature rise can be approximated as $\Delta T = \frac{2\alpha I \Delta t}{\rho C}$, where Δt is the total exposure time, *C* the heat capacity, and ρ the tissue density. Because $\alpha \propto f$, the effects of heating increase with ultrasound frequency (Figure 2). Moreover, the equation shows that heating only depends on the amount of delivered energy and is PRF independent (Figure 2, red).

Several studies have suggested that ultrasonic stimulation of the nervous system is more effective at lower frequencies (33,35,76–79), which corroborates the engagement of either particle displacement or a stable cavitation-related mechanism. All 4 mechanisms engage membranes, neurons, astrocytes (80), synaptic vesicles, and likely also other excitable and passive structures (81–87).

Safety

For ultrasound imaging, which uses pulses on the order of microseconds, the Food and Drug Administration (FDA) (72) defined limits on MI and peak acoustic intensity I_{SPPA} to prevent mechanical damage and on time-average intensity I_{SPTA} to prevent thermal damage, where SPPA is spatial-peak pulse-average and SPTA is spatial-peak temporal-average. ITRUSST (International Transcranial Ultrasonic Stimulation Safety and Standards Consortium) has recently provided recommendations to prevent mechanical and thermal damage for neuromodulation (73), which uses pulse durations on the order of dozens of milliseconds. Consistent with the FDA, the consortium agreed that operations within MI$<$1.9 are associated with a nonsignificant risk of harmful cavitation and mechanical damage. To prevent thermal damage, the consortium recommends that operators comply with at least one of the following: 1) a temperature rise $<$2 °C, 2) a thermal dose $<$0.25 in CEM43 units, or 3) specific values of the thermal index for a given exposure time (73). The consortium also provided conservative (95th percentile) values that can be used to derate the ultrasound attenuation by the human skull (88). Investigators are urged to measure or at least approximate these metrics before attempting any therapy (73,88).

CLINICAL APPLICATIONS

The following sections describe applications of ultrasonic neuromodulation to affective disorders, schizophrenia, chronic pain, and disorders of consciousness (DOC). Multiple randomized sham-controlled trials (RCTs) have demonstrated improvements that are superior to sham. All studies applied ultrasound within MI$<$1.9. Side effects were rare and likely unrelated to stimulation, as noted below.

Major Depression

Two groups targeted the subcallosal cingulate cortex (SCC) based on recent discoveries in the deep brain stimulation literature (89). SCC stimulation, but not unfocused stimulation, significantly improved ratings of depression and anxiety in 2 participants with treatment-resistant depression (42). In a follow-up study, the same group applied ultrasound to 3 distinct subregions of the anterior cingulate cortex (ACC) and found that improvements in depression were strongest when targeting the SCC (90). Beneficial effects were observed up until the last evaluation point, 44 days following the stimulation. A subsequent RCT recruited 22 patients with treatment-resistant depression (44). The study acquired fMRI blood oxygen level–dependent (BOLD) signals during stimulation and found significant engagement of the SCC target in 7 of 16 participants. There were significant improvements in the Hamilton Depression Rating Scale scores in the per-protocol sample of 19 patients. Another group targeted the SCC in an open-label study involving 5 patients with treatment-resistant depression (91). Stimulation targeting the intersection of white matter tracts (89) was delivered in 5 sessions/day for 5 days, and harnessed an acoustic metalens to mitigate the defocusing of ultrasound through the skull. Improvements in depressive symptoms were observed for up to 5 weeks following the stimulation.

Stimulation has also been applied to other regions. Five-minute stimulation of the anterior nucleus of the thalamus led to significant improvements in depressive symptoms compared with stimulation of the ventral capsule and the bed nucleus of the stria terminalis and unfocused stimulation (92). An open-label study modulated the amygdala in 15 active sessions over 3 weeks in 29 participants with mood, anxiety, and trauma-related disorders (45). The stimulation reduced the fMRI BOLD signal in the target and improved mood and anxiety symptoms. A randomized sham-controlled study applied stimulation to the left dorsolateral prefrontal cortex (DLPFC) of 26 patients with major depression in 6 sessions over 2 weeks (93). There were notable improvements in depressive symptoms, which were observed at the end of the treatment regimen and were even stronger 2 weeks posttreatment. Another study conducted an RCT that delivered six 30-minute sessions of brief high-intensity ultrasound pulses to the DLPFC of 30 participants. There was a substantial decrease in depressive symptoms and improvements in cognitive metrics following the intervention and at the 3-month follow-up (94).

One study found worsening of depressive symptoms in 2 participants, although the worsening was delayed and appeared stimulation unrelated (44).

Anxiety

In a feasibility study, 8 weekly 10-minute stimulation sessions were delivered targeting the right amygdala in 25 patients with generalized anxiety disorder (95). Many patients experienced substantial improvements in the Hamilton Anxiety Rating Scale scores. In a subsequent double-blind RCT, the stimulation was applied once per week over 4 weeks (96).

Schizophrenia

A pilot study tested the potential of using ultrasound for treatment of schizophrenia (97). Fifteen sessions of 15-minute stimulation were delivered to the left DLPFC in 26 patients. The study found significant intervention-condition interactions for the Positive and Negative Syndrome Scale and the Scale for the Assessment of Negative Symptoms.

Chronic Pain

Studies of healthy individuals suggest that ultrasonic stimulation may be able to modulate pain perception (98,99). In an initial RCT, 15 seconds of stimulation was applied using a high-frequency imaging probe to the posterior frontal cortex in 31 patients with chronic pain (100). Compared with placebo, there were significant improvements in mood and global affect at 10 and 40 minutes following stimulation and a trend toward a decrease in pain intensity. In another RCT, 40 minutes of ultrasonic stimulation was applied to the ACC of 20 patients with chronic pain (101). There was a 60% decrease in pain intensity immediately following the treatment. Clinically meaningful effects were observed up to 7 days following the

stimulation. Sham stimulation, which delivered auditory masking sounds, provided minor benefits. The ACC was also stimulated in an open-label study, 3 times a week for 2 weeks (up to 30 min/session) in 11 patients with neuropathic pain (102). There were significant improvements in pain intensity for up to 4 weeks following the stimulation.

Disorders of Consciousness

Ultrasonic stimulation holds promise for noninvasive modulation of arousal and treatments of DOC (103). A patient with posttraumatic DOC received 10 epochs of 30-second stimulation of the central thalamus (104). The patient was responsive on day 3 following the stimulation and attempted to walk on day 5. Stimulation of the central thalamus over 2 sessions found clinically significant increases in behavioral responsiveness in 2 of 3 participants (105). In a subsequent study, stimulation was applied to 11 patients with acute DOC (41). The was a significant and rapid effect on the Coma Recovery Scale. Repeated treatments over 2 to 4 years with brief high-intensity pulses applied nonselectively to the brain improved specific coma scores (106). Although these results are encouraging, all studies lacked a sham condition. Two adverse events occurred in patients with DOC; both were considered unrelated to the stimulation (41).

Summary of Current Clinical Applications

Despite these promising results, the current RCTs are relatively small and have targeted various conditions using various brain regions and ultrasound parameters. Therefore, there is no consensus and there are no specific guidelines on the most suitable application of this emerging technology. Guidelines on the important factors that should be considered when designing and conducting such studies are provided below.

GUIDELINES

Causal Brain Mapping to Identify the Involved Brain Regions

The review of current clinical studies highlighted the potential of ultrasonic neuromodulation for circuit-directed treatments. However, circuit-directed treatments of mental and neurological disorders are limited by two key issues: 1) the brain circuits associated with most disorders are not well understood, and 2) there is typically appreciable variability from individual to individual (107). The ultrasound provides a potentially powerful approach for addressing these issues, enabling the mapping of circuit function in a causal manner for the first time. By systematically and reversibly perturbing individual candidate regions, it is possible to establish their role in the studied behaviors and disease signs.

In this approach, brief ultrasound stimulation is systematically applied (step 1 in Figure 3A) to a set of targets (Figure 3B, C). The duration of the stimulation is titrated to elicit transient changes in disease symptoms. Regions that maximize improvements in disease symptoms (purple rectangles, step 2) are subsequently selected for sustained stimulation (step 3, Figure 3D, E). This method has the potential to provide personalized therapies.

Parameters That Maximize Neuromodulatory Effects

Some studies suggest that ultrasonic stimulation of the nervous system is more effective at lower frequencies (33,35,76–79), while others suggest the opposite (51,52). This dichotomy is likely due to the distinct classes of mechanisms invoked at distinct frequencies (Figure 2). Nevertheless, for applications to psychiatric and neurological disorders, the ultrasound must propagate through the human skull, which confines the frequency range to about 0.2 to 0.8 MHz (Figure 2, green) (29–31,48).

As expected, the effects of ultrasonic neuromodulation increase monotonically with increasing intensity I (32–36,50–52,55–57,76,108,109).

The effects also increase monotonically with increasing duration of the ultrasound pulse, t_{ON} (52,54,62,76,108,110). This parameter may have broad explanatory power. For example, the effect of t_{ON} can parsimoniously explain the rich findings of a recent study that investigated the effects of individual parameters on many neuronal types (109). The pulse duration t_{ON} explains the prominent effect of the PRF (the optimal value of 2.5-Hz PRF is associated with the longest t_{ON}). The pulse duration t_{ON} also captures the effect of the duty cycle (the optimal value of 20% duty cycle is associated with the longest t_{ON}).

Because neuromodulatory effects commonly follow strength-duration relationships (111), we may expect a multiplicative relationship between I and t_{ON}. There is indeed evidence for a multiplicative interaction (52,76,110). Thus, the neuromodulatory effects of ultrasound E, quantified on neurons or behavior, scale as $E \propto It_{ON}$ (Figure 4A, black arrow). Generalized to $E \propto \int I(t)dt$, E constitutes the total stimulation energy per unit area.

At the same time, E must be curbed to comply with safety guidelines. Here, I_{SPTA} serves as a useful constraint on the energy delivered over time. Defined as $I_{SPTA} = I\frac{t_{ON}}{t_T}$, where t_T is the time between individual pulses of ultrasound, I_{SPTA} is capped at a certain value (e.g., the 510(k) Track 3 imaging guidelines pose a limit of $I_{SPTA} < 720$ mW/cm^2). Given this limit, the space of the applicable intensities and pulse durations is confined to an area below a hyperbolic curve given by the relationship $I = \frac{I_{SPTA}t_T}{t_{ON}}$ (Figure 4A). Because $I = \frac{I_{SPTA}t_T}{t_{ON}}$ and $E \propto It_{ON}$, it follows that $E \propto I_{SPTA}t_T$. Thus, the effectiveness of ultrasonic neuromodulation scales with I_{SPTA}. In the common case of operation near or at a regulatory limit (e.g., $I = I_{SPTA} =$ 720 mW/cm^2), the equation suggests that the effect E can be maximized by using a relatively long time t_T between the individual ultrasound pulse durations (see 4 example values in Figure 4A). This strategy has been applied in recent clinical studies (44,101).

From $E \propto I_{SPTA}t_T$, the magnitude of effects E is defined and capped by I_{SPTA} (dashed red contours in Figure 4A). This is a useful constraint given that the red dashed lines also represent equipotential values of E (notice that $I \propto \frac{E}{t_{ON}}$). These considerations condense the initially 2-dimensional space of I and t_{ON} into a 1-dimensional space parameterized by a single value along each curve for a given t_T.

Finally, within each pulse, the ultrasound can be pulsed with a specific PRF and at a specific duty cycle value. These two parameters are especially pertinent in high-frequency applications (Figure 2). Radiation force–based effects are

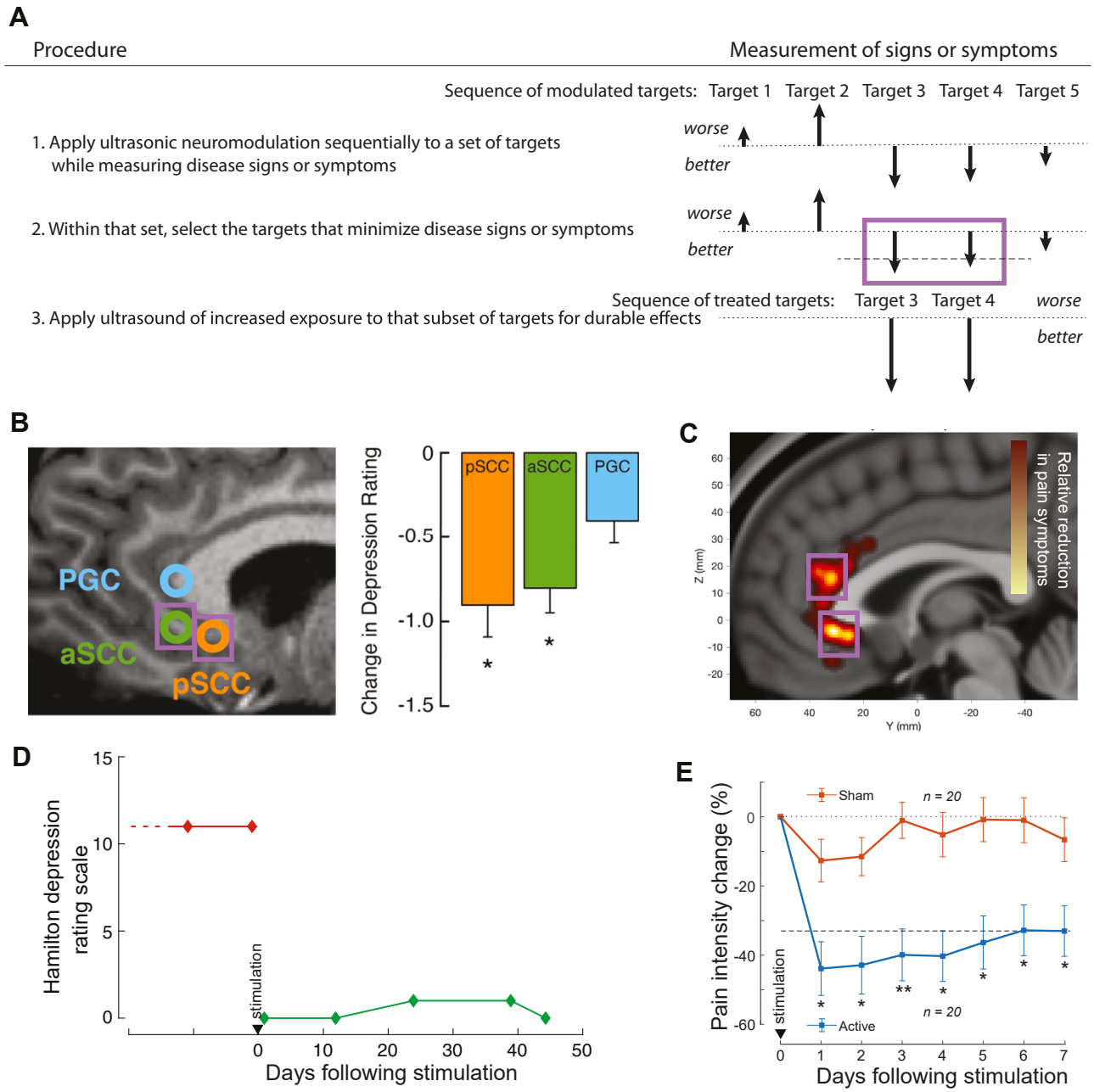

Figure 3. Circuit-directed individualized treatments. **(A)** In this example, ultrasonic neuromodulation is sequentially applied, one by one, to 5 brain targets. Disease signs are measured during and immediately after the neuromodulation of each target. Changes in measured values are indicated as arrows with certain length (the longer the upward arrow, the worse the signs or symptoms; the longer the downward arrow, the better the signs or symptoms). The dotted line provides a baseline state of the disease signs (no change) prior to any intervention. Next (step 2), an operator or an algorithm selects the targets that minimize the disease signs or exceed a predefined threshold of improvement or a statistical criterion. The dashed line exemplifies a threshold for the selection of a substantial improvement. In this example, target 3 and target 4 are selected (thick rectangle). Finally, ultrasound of increased exposure is applied (step 3) to the selected targets 3 and 4. This higher-energy intervention aims to improve signs even more (long downward arrows) and provide relief that is more durable. **(B)** Examples of target-dependent changes in mood. Three targets were stimulated repeatedly in a participant with treatment-resistant depression: the pregenual cingulate (PGC), anterior subcallosal cingulate cortex (aSCC), and posterior SCC (pSCC). Sagittal view is shown. Ultrasound stimuli (90) were delivered in a randomized order under blind conditions, separated by 1-minute rest periods. After each trial, the participant rated subjective change in mood during that trial on a −3 to +3 scale. Mean ± SEM ratings are shown (10 trials/target). *$p < .05$, one-sample t test. **(C)** Immediate changes in numerical rating scale of pain in response to consecutive stimulation of 8 subregions of the anterior cingulate cortex (ACC) (101). **(D)** Changes in depressive symptoms following the delivery of the ultrasound to the SCC in the same participant (90). **(E)** Changes in depressive symptoms following the delivery of the ultrasound to the dorsal and ventral portions of the ACC in 20 participants (101). **$p < .01$.

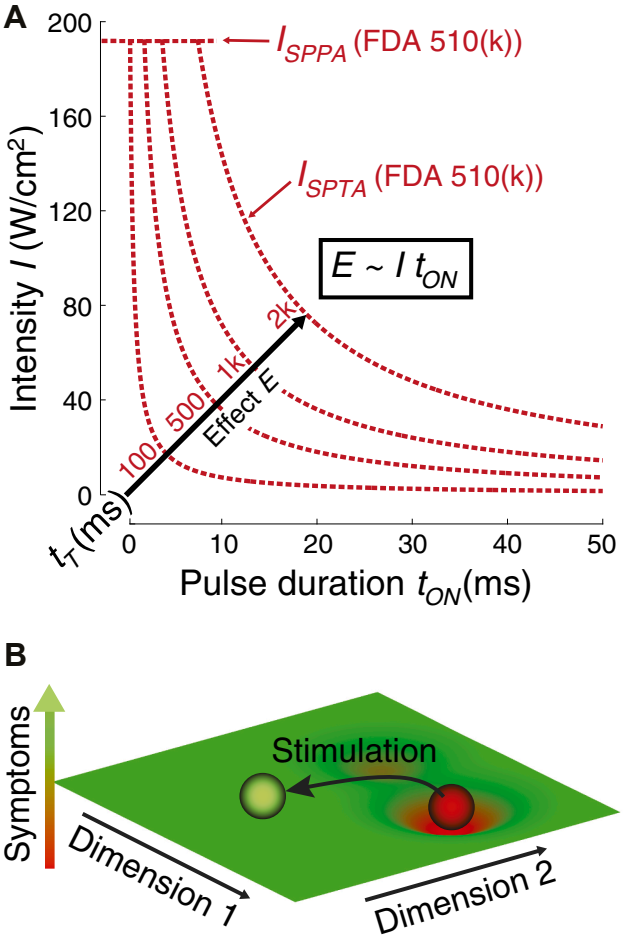

Figure 4. Stimulation parameters and sustained effects. **(A)** The selection of effective and safe parameters. The effects of ultrasonic neuromodulation scale with the ultrasound intensity and pulse duration, $E \propto It_{ON}$ (black arrow). At the same time, stimulation is subject to a safety value that prevents excessive energy deposition, $I_{SPTA} = \frac{It_{ON}}{t_T}$, where t_T is the interpulse duration interval, i.e., $t_T = t_{ON} + t_{OFF}$. The red dashed hyperbolae are computed for $I_{SPTA} = 720$ mW/cm^2 (72) used for 510(k) clearance of ultrasound imaging systems. Text in red shows 4 specific values of t_T. Since $E \propto It_{ON}$ and so $I \propto \frac{E}{t_{ON}}$, the hyperbolae also represent equipotential levels of E. Thus, taking both effectiveness and safety into account, the space of stimulation parameters can be substantially reduced. For completeness, the figure also provides the value of $I_{SPPA} < 190$ W/cm^2 (72) used for 510(k) clearance of ultrasound imaging systems. **(B)** Sustained effects: A dynamical system view. In this view, neural network dysfunction is represented by extrema in a multidimensional system representation. The individual dimensions may represent neural activity of individual network nodes, the strength of connections between them, or both. Stimulation can rapidly tip the system out of an undesirable extremum (red) into a desirable and potentially stable state (green). The system is dynamic: The attractor landscape can change over time as a function of many factors including adjuvant therapies. For visualization purposes, only 2 principal dimensions of a system are shown. FDA, Food and Drug Administration; SPPA, spatial-peak pulse-average; SPTA, spatial-peak temporal-average.

sensitive to the PRF (51,69,70). By definition, heating effects are insensitive to PRF but sensitive to duty cycle, as higher values of duty deliver more energy into the target. These two additional parameters may also matter during low-frequency stimulations that could be delivered through the human head (76,79,112) (Figure 2, purple).

Accounting for Skull and Hair

The attenuation of ultrasound by the skull (Figure 5A) constitutes a key factor in the ultrasound intensity delivered into the brain (113). A meta-analysis suggests that this factor likely resulted in inadequate intensity in early human neuromodulation studies (Figure 5B). Imaging and simulations have been relatively unsuccessful in accounting for the attenuation of ultrasound by the skull. There is no consistent relationship between computed tomography or MR image parameters and acoustic attenuation (114–117). Moreover, repeated applications of neuromodulation to psychiatric and chronic conditions introduce an additional layer of complexity—the hair. The hair entraps ultrasound-reflecting bubbles, thus dampening the delivered intensity further and substantially (113).

On this front, MRI acoustic radiation force imaging (ARFI) (118–120) is an emerging ultrasound guidance method that also has the potential to estimate the delivered intensity (118,121).

In addition, the attenuation and dephasing can be directly measured using ultrasound itself applied in a relative through-transmission manner (113,122). In this method, brief pulses of low-intensity ultrasound are emitted from an element through the coupling media, hair, skull, and head. Responses are gathered on elements of the opposite array. By comparing the amplitude and timing of the received waveforms with those obtained in water, a compensation algorithm can appropriately set the amplitude and timing of ultrasound emission from each array element, and thus deliver the desired intensity into the desired target (113).

Target Engagement

Target engagement confirms a physiological response of the stimulated neural tissue, and can be evaluated using fMRI (Figure 1A), effects on behavior (Figure 1B), or electrophysiological approaches such as electroencephalography (81–87,117,123). For ultrasound, which commonly targets deep brain structures, MRI offers a unique tool for volumetric imaging at depth. Several studies have shown modulation of fMRI BOLD activity (45) by neuromodulatory ultrasound. The effects include both a decrease (41,43–45,113) (Figure 1A) and an increase (124,125) in the BOLD signal (126). The depth of modulation (Figure 1A, bottom) could potentially serve as a readout of the target engagement magnitude. Ultrasound also modulates resting-state BOLD connectivity between the stimulated target and associated regions (127–131).

Induction of Sustained Effects

The clinical studies reviewed in this article suggest that the neuromodulatory effects of ultrasound can provide benefits that range from days to months following a stimulation regimen. Mechanistically, it is known that ultrasound engages glial cells and thus modulates synaptic events (80,132), but the associated neuroplastic effects generally only last from minutes to hours (127,133).

A conceptual explanation for the durable effects of ultrasound observed in clinical studies makes use of a dynamical

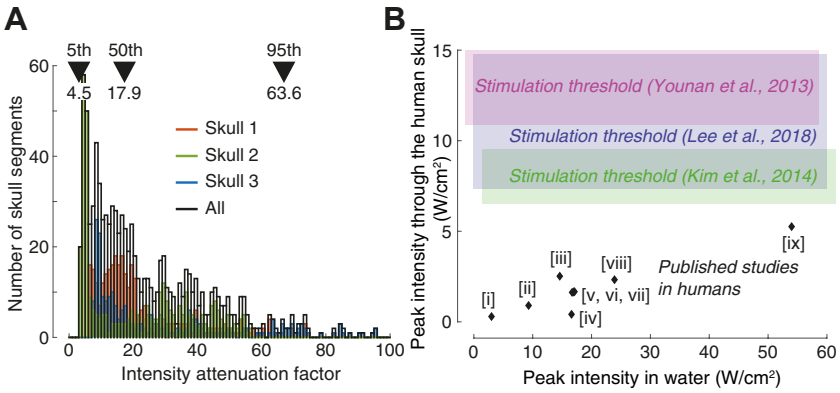

Figure 5. The human skull has led to inadequate ultrasonic stimulation. **(A)** Histogram of ultrasound intensity attenuation measured across 3 × 360 segments in 3 human ex vivo skulls (139). The figure shows strong attenuation of ultrasound intensity (a factor of 17.9, median) and high variability within and across individuals. **(B)** Meta-analysis of early human neuromodulation studies that measured target intensity in water (abscissa). The ordinate provides actually delivered intensities through the respective parts of the human skull using measured attenuation values through those skull parts (139). The resulting values are below the stimulation threshold ranges (in color) established in rodent studies (33,73,140). The inset roman numerals tie to (47,141–148) in this order.

system view (Figure 4B). It is now appreciated that neuropsychiatric conditions such as depression are associated with aberrant patterns of network activity and connectivity, as opposed to the failure of single regions (14–20). Because a network involves multiple nodes and connections, a multidimensional view must be taken to fully characterize these complex systems. In this view, a disorder is seen as an extremum or extrema in this multidimensional dynamical system representation (red in Figure 4B). An ultrasonic intervention of sufficient energy (Figure 4A) may be able to tip the system out of an extremum (green in Figure 4B). If the disease-related extrema are relatively sparse, as shown in Figure 4B, the resulting improvements may be stable.

As a specific example, depression is believed to be associated with hyperactive (Figure 4B, dimension 1) and hyperconnected (dimension 2) SCC (14–16). Directing ultrasound into that target (Figure 1A) can suppress its hyperactivity (44) and hyperconnectivity (131). The resulting improvements in depressive symptoms may be sustained for a clinically relevant duration (Figure 3D).

CONFOUNDS

Ultrasound can cause auditory perception in humans (134) and rodents (135). This issue is particularly notable in rodents (136), where the small cranium conducts ultrasound with little attenuation into auditory and vestibular structures. Moreover, the wavelength for human-applicable frequencies (Figure 2) is large with respect to the small cranium, which leads to standing waves (136), notable reflections throughout the brain, and a multitude of potential artifacts (135,137).

There are several effective strategies to minimize these artifacts. First, the onset and offset of each pulse duration can be smoothed to eliminate sudden changes and thus auditory perception (138). Second, proper sham stimulation can be provided by delivering sounds through earphones, such that participants cannot distinguish verum from sham stimulation (134). Third, the ultrasound can be applied in an unfocused manner (92,113) or to an inactive site as a negative control. Any new study in the field, whether basic or translational, should use at least one of these strategies to control for potential confounds.

SUMMARY AND OUTLOOK

This review highlights the progress that the field of ultrasonic neuromodulation has made over the past several years. The recent growth has been fueled by MRI-based approaches for precision guidance and methods that compensate for the distortions of ultrasound by the human skull. The emergence of RCTs demonstrates that the field is moving rapidly toward clinical applications.

This article provides guidance for applying ultrasonic neuromodulation to the human brain effectively and safely. The neuromodulatory effects are found to scale with intensity and pulse duration as key parameters: $E \propto I t_{ON}$. A review of mechanistic findings intersected with safety indices and skull constraints leads to the conclusion that the 5-dimensional space of parameters can be effectively reduced to 2 to 3 dimensions, thus making the search for optimal stimulation parameters for a particular disorder tractable.

Future research will reveal submechanisms of the 4 major categories. Researchers and clinicians will use this knowledge to fine-tune the stimulation parameters for a specific neuromodulation purpose. Future work will also elucidate the concepts and mechanisms that produce sustained effects, including effects on neuroplasticity and equilibria of dynamical neural networks. The skull, hair, and coupling will be adequately compensated for using increasingly sophisticated simulations and through-transmission approaches. MRI ARFI will provide reliable images of the ultrasound target deep in the brain and possibly inform on the delivered intensity. fMRI BOLD and associated readouts will provide robust maps of physiological target engagement. The full power of the noninvasiveness and flexible delivery will be harnessed using systematic and personalized approaches (Figure 3). Ultimately, these technological and conceptual advances will lead to circuit-directed and personalized therapies for the many patients who are currently out of options.

ACKNOWLEDGMENTS AND DISCLOSURES

This work was supported by the National Science Foundation (Grant No. CBET 2325125 [to JK]), the National Institutes of Health (Grant No. R61/R33 [1R61MH134943] [to JK]), and Wellcome Leap Untangling Addiction (to JK).

JK is an inventor, cofounder, and consultant for SPIRE Therapeutics Inc.

ARTICLE INFORMATION

From the Departments of Psychiatry, Neurology, Radiology, and Biomedical Engineering, Washington University School of Medicine, St. Louis, Missouri (JK).

Address correspondence to Jan Kubanek, Ph.D., at kubanek@wustl.edu.

Received Sep 22, 2025; revised Jan 5, 2026; accepted Jan 17, 2026.

REFERENCES

1. The Lancet (2017): Life, death, and disability in 2016. Lancet 390:1083.
2. Ahrnsbrak R, Bose J, Hedden S, Lipari R, Park-Lee E (2017): Key Substance Use and Mental Health Indicators in the United States: Results From the 2016 National Survey on Drug Use and Health. Rockville, MD: Center for Behavioral Health Statistics and Quality, Substance Abuse and Mental Health Services Administration.
3. Posse PR, Nemeroff CB (2012): The problem of treatment-resistant psychiatric disorders. In: Nemeroff CB, editor. Management of Treatment-Resistant Major Psychiatric Disorders. Oxford, England: Oxford University Press, 3–22.
4. Al-Harbi KS (2012): Treatment-resistant depression: Therapeutic trends, challenges, and future directions. Patient Preference Adherence 6:369–388.
5. Jaffe DH, Rive B, Denee TR (2019): The humanistic and economic burden of treatment-resistant depression in Europe: A cross-sectional study. BMC Psychiatry 19:247.
6. Bystritsky A (2006): Treatment-resistant anxiety disorders. Mol Psychiatry 11:805–814.
7. Hamner MB, Robert S, Frueh BC (2004): Treatment-resistant post-traumatic stress disorder: Strategies for intervention. CNS Spectr 9:740–752.
8. Freire RC, Zugliani MM, Garcia RF, Nardi AE (2016): Treatment–resistant panic disorder: A systematic review. Expert Opin Pharmacother 17:159–168.
9. Ferguson JM (2001): SSRI antidepressant medications: Adverse effects and tolerability. Prim Care Companion J Clin Psychiatry 3:22–27.
10. Lindenmayer JP (2000): Treatment refractory schizophrenia. Psychiatr Q 71:373–384.
11. Widge AS, Dougherty DD (2015): Deep brain stimulation for treatment-refractory mood and obsessive-compulsive disorders. Curr Behav Neurosci Rep 2:187–197.
12. Organization WH (2009): Pharmacological Treatment of Mental Disorders in Primary Health Care. Geneva, Switzerland: World Health Organization.
13. Guery D, Rheims S (2021): Clinical management of drug resistant epilepsy: A review on current strategies. Neuropsychiatr Dis Treat 17:2229–2242.
14. Morris LS, Costi S, Tan A, Stern ER, Charney DS, Murrough JW (2020): Ketamine normalizes subgenual cingulate cortex hyper-activity in depression. Neuropsychopharmacology 45:975–981.
15. Johansen-Berg H, Gutman DA, Behrens TE, Matthews PM, Rushworth MF, Katz E, *et al.* (2008): Anatomical connectivity of the subgenual cingulate region targeted with deep brain stimulation for treatment-resistant depression. Cereb Cortex 18:1374–1383.
16. Rodríguez-Cano E, Sarró S, Monté GC, Maristany T, Salvador R, McKenna PJ, Pomarol-Clotet E (2014): Evidence for structural and functional abnormality in the subgenual anterior cingulate cortex in major depressive disorder. Psychol Med 44:3263–3273.
17. Alexander L, Clarke HF, Roberts AC (2019): A focus on the functions of area 25. Brain Sci 9:129.
18. Davidson RJ (2002): Anxiety and affective style: Role of prefrontal cortex and amygdala. Biol Psychiatry 51:68–80.
19. Bishop SJ (2007): Neurocognitive mechanisms of anxiety: An integrative account. Trends Cogn Sci 11:307–316.
20. Tye KM, Prakash R, Kim SY, Fenno LE, Grosenick L, Zarabi H, *et al.* (2011): Amygdala circuitry mediating reversible and bidirectional control of anxiety. Nature 471:358–362.
21. Perlmutter JS, Mink JW (2006): Deep brain stimulation. Annu Rev Neurosci 29:229–257.
22. Kellner CH, Greenberg RM, Murrough JW, Bryson EO, Briggs MC, Pasculli RM (2012): ECT in treatment-resistant depression. Am J Psychiatry 169:1238–1244.
23. Arle J, Shils JL (2017): Innovative Neuromodulation. Cambridge, England: Academic Press.
24. Kisely S, Li A, Warren N, Siskind D (2018): A systematic review and meta-analysis of deep brain stimulation for depression. Depress Anxiety 35:468–480.
25. Meeres J, Hariz M (2022): Deep brain stimulation for post-traumatic stress disorder: A review of the experimental and clinical literature. Stereotact Funct Neurosurg 100:143–155.
26. Antal A, Paulus W (2013): Transcranial alternating current stimulation (tACS). Front Hum Neurosci 7:317.
27. Brunoni AR, Nitsche MA, Bolognini N, Bikson M, Wagner T, Merabet L, *et al.* (2012): Clinical research with transcranial direct current stimulation (tDCS): Challenges and future directions. Brain Stimul 5:175–195.
28. Soroushi H, Abbasi S, Du Y, Ning N, Lei Y (2025): Temporal interference stimulation: Mechanisms, optimization, validation, and clinical prospects—A comprehensive review. WIREs Computational Stats 17:e70031.
29. Hynynen K, Jolesz FA (1998): Demonstration of potential noninvasive ultrasound brain therapy through an intact skull. Ultrasound Med Biol 24:275–283.
30. Sun J, Hynynen K (1999): The potential of transskull ultrasound therapy using the maximum available skull surface area. J Acoust Soc Am 105:2519–2527.
31. Sun J, Hynynen K (1998): Focusing of therapeutic ultrasound through a human skull: A numerical study. J Acoust Soc Am 104:1705–1715.
32. Lee W, Croce P, Margolin RW, Cammalleri A, Yoon K, Yoo SS (2018): Transcranial focused ultrasound stimulation of motor cortical areas in freely-moving awake rats. BMC Neurosci 19:57.
33. Tufail Y, Matyushov A, Baldwin N, Tauchmann ML, Georges J, Yoshihiro A, *et al.* (2010): Transcranial pulsed ultrasound stimulates intact brain circuits. Neuron 66:681–694.
34. Kamimura HAS, Wang S, Chen H, Wang Q, Aurup C, Acosta C, *et al.* (2016): Focused ultrasound neuromodulation of cortical and subcortical brain structures using 1.9 MHz. Med Phys 43:5730.
35. Ye PP, Brown JR, Pauly KB (2016): Frequency dependence of ultrasound neurostimulation in the mouse brain. Ultrasound Med Biol 42:1512–1530.
36. Li GF, Zhao HX, Zhou H, Yan F, Wang JY, Xu CX, *et al.* (2016): Improved anatomical specificity of non-invasive neuro-stimulation by high frequency (5 MHz) ultrasound. Sci Rep 6:24738.
37. Riis TS, Losser AJ, Kassavetis P, Moretti P, Kubanek J (2024): Noninvasive modulation of essential tremor with focused ultrasonic waves. J Neural Eng 21:016033.
38. Bancel T, Béranger B, Daniel M, Didier M, Santin M, Rachmilevitch I, *et al.* (2024): Sustained reduction of essential tremor with low-power non-thermal transcranial focused ultrasound stimulations in humans. Brain Stimul 17:636–647.
39. Deveney CM, Surya JR, Haroon JM, Mahdavi KD, Hoffman KR, Enemuo KC, *et al.* (2024): Transcranial focused ultrasound for the treatment of tremor: A preliminary case series. Brain Stimul 17:35–38.
40. Kiss Z, Arantes A, Adeoti J, Coreas A, Sheth N, Swytink-Binnema C, *et al.* (2025): Tremor reduction using multi-focus transcranial ultrasound stimulation system targeting thalamus: Preliminary results. Brain Stimul 18:610.
41. Cain JA, Spivak NM, Coetzee JP, Crone JS, Johnson MA, Lutkenhoff ES, *et al.* (2022): Ultrasonic deep brain neuromodulation in acute disorders of consciousness: A proof-of-concept. Brain Sci 12:428.
42. Riis T, Feldman D, Losser A, Mickey B, Kubanek J (2024): Device for multifocal delivery of ultrasound into deep brain regions in humans. IEEE Trans Biomed Eng 71:660–668.

43. Peng X, Connolly DJ, Sutton F, Robinson J, Baker-Vogel B, Short EB, Badran BW (2024): Non-invasive suppression of the human nucleus accumbens (NAc) with transcranial focused ultrasound (tFUS) modulates the reward network: A pilot study. Front Hum Neurosci 18:1359396.
44. Riis TS, Feldman DA, Kwon SS, Vonesh LC, Koppelmans V, Brown JR, *et al.* (2025): Noninvasive modulation of the subcallosal cingulate and depression with focused ultrasonic waves. Biol Psychiatry 97:825–834.
45. Barksdale BR, Enten L, DeMarco A, Kline R, Doss MK, Nemeroff CB, Fonzo GA (2025): Low-intensity transcranial focused ultrasound amygdala neuromodulation: A double-blind sham-controlled target engagement study and unblinded single-arm clinical trial. Mol Psychiatry 30:4497–4511.
46. Lee W, Kim HC, Jung Y, Chung YA, Song IU, Lee JH, Yoo SS (2016): Transcranial focused ultrasound stimulation of human primary visual cortex. Sci Rep 6:34026.
47. Wilson MG, Riis TS, Kubanek J (2024): Controlled ultrasonic interventions through the human skull. Front Hum Neurosci 18:1412921.
48. Fry FJ, Barger JE (1978): Acoustical properties of the human skull. J Acoust Soc Am 63:1576–1590.
49. Tyler WJ, Tufail Y, Finsterwald M, Tauchmann ML, Olson EJ, Majestic C (2008): Remote excitation of neuronal circuits using low-intensity, low-frequency ultrasound. PLoS One 3:e3511.
50. Kubanek J, Shi J, Marsh J, Chen D, Deng C, Cui J (2016): Ultrasound modulates ion channel currents. Sci Rep 6:24170.
51. Kubanek J, Shukla P, Das A, Baccus SA, Goodman MB (2018): Ultrasound elicits behavioral responses through mechanical effects on neurons and ion channels in a simple nervous system. J Neurosci 38:3081–3091.
52. Menz MD, Ye P, Firouzi K, Nikoozadeh A, Pauly KB, Khuri-Yakub P, Baccus SA (2019): Radiation force as a physical mechanism for ultrasonic neurostimulation of the ex vivo retina. J Neurosci 39:6251–6264.
53. Hoffman BU, Baba Y, Lee SA, Tong CK, Konofagou EE, Lumpkin EA (2022): Focused ultrasound excites action potentials in mammalian peripheral neurons in part through the mechanically gated ion channel PIEZO2. Proc Natl Acad Sci U S A 119:e2115821119.
54. Zhu J, Xian Q, Hou X, Wong KF, Zhu T, Chen Z, *et al.* (2023): The mechanosensitive ion channel Piezo1 contributes to ultrasound neuromodulation. Proc Natl Acad Sci U S A 120: e2300291120.
55. Matsushita Y, Yoshida K, Yoshiya M, Shimizu T, Tsukamoto S, Kudo N, *et al.* (2024): TRPC6 is a mechanosensitive channel essential for ultrasound neuromodulation in the mammalian brain. Proc Natl Acad Sci U S A 121:e2404877121.
56. Sorum B, Rietmeijer RA, Gopakumar K, Adesnik H, Brohawn SG (2021): Ultrasound activates mechanosensitive TRAAK K+ channels through the lipid membrane. Proc Natl Acad Sci U S A 118: e2006980118.
57. Sorum B, Docter T, Panico V, Rietmeijer RA, Brohawn SG (2024): Tension activation of mechanosensitive two-pore domain K+ channels TRAAK, TREK-1, and TREK-2. Nat Commun 15:3142.
58. Prieto ML, Maduke M (2024): Towards an ion-channel-centric approach to ultrasound neuromodulation. Curr Opin Behav Sci 56:101355.
59. Ye J, Tang S, Meng L, Li X, Wen X, Chen S, *et al.* (2018): Ultrasonic control of neural activity through activation of the mechanosensitive channel MscL. Nano Lett 18:4148–4155.
60. Cadoni S, Demené C, Alcala I, Provansal M, Nguyen D, Nelidova D, *et al.* (2023): Ectopic expression of a mechanosensitive channel confers spatiotemporal resolution to ultrasound stimulations of neurons for visual restoration. Nat Nanotechnol 18:667–676.
61. Duque M, Lee-Kubli CA, Tufail Y, Magaram U, Patel J, Chakraborty A, *et al.* (2022): Sonogenetic control of mammalian cells using exogenous Transient Receptor Potential A1 channels. Nat Commun 13:600.
62. Vasan A, Orosco J, Magaram U, Duque M, Weiss C, Tufail Y, *et al.* (2022): Ultrasound mediated cellular deflection results in cellular depolarization. Adv Sci (Weinh) 9:e2101950.
63. Roovers S, Segers T, Lajoinie G, Deprez J, Versluis M, De Smedt SC, Lentacker I (2019): The role of ultrasound-driven microbubble dynamics in drug delivery: From microbubble fundamentals to clinical translation. Langmuir 35:10173–10191.
64. Plaksin M, Shoham S, Kimmel E (2014): Intramembrane cavitation as a predictive bio-piezoelectric mechanism for ultrasonic brain stimulation. Phys Rev X 4:011004.
65. Plaksin M, Kimmel E, Shoham S (2016): Cell-type-selective effects of intramembrane cavitation as a unifying theoretical framework for ultrasonic neuromodulation. eNeuro 3:ENEURO.0136-15.2016.
66. Tarnaud T, Joseph W, Schoeters R, Martens L, Tanghe E (2021): Membrane charge oscillations during ultrasonic neuromodulation by intramembrane cavitation. IEEE Trans Biomed Eng 68:2892–2903.
67. Apfel RE, Holland CK (1991): Gauging the likelihood of cavitation from short-pulse, low-duty cycle diagnostic ultrasound. Ultrasound Med Biol 17:179–185.
68. Cobbold RSC (2006): Foundations of Biomedical Ultrasound. Oxford, England: Oxford University Press.
69. Yu K, Niu X, Krook-Magnuson E, He B (2021): Intrinsic functional neuron-type selectivity of transcranial focused ultrasound neuromodulation. Nat Commun 12:2519.
70. Ramachandran S, Gao H, Yttri E, Yu K, He B (2025): Parameter-dependent cell-type specific effects of transcranial focused ultrasound stimulation in an awake head-fixed rodent model. J Neural Eng 22:026022.
71. Xu K, Yang Y, Hu Z, Yue Y, Gong Y, Cui J, *et al.* (2023): TRPV1-mediated sonogenetic neuromodulation of motor cortex in freely moving mice. J Neural Eng 20:016055.
72. U.S. Food and Drug Administration (2023): Marketing clearance of diagnostic ultrasound systems and transducers. Available at: https://www.fda.gov/media/71100/download.
73. Aubry JF, Attali D, Schafer ME, Fouragnan E, Caskey CF, Chen R, *et al.* (2025): ITRUSST consensus on biophysical safety for transcranial ultrasound stimulation. Brain Stimul 18:1896–1905.
74. Downs ME, Lee SA, Yang G, Kim S, Wang Q, Konofagou EE (2018): Non-invasive peripheral nerve stimulation via focused ultrasound in vivo. Phys Med Biol 63:035011.
75. Yang Y, Yuan J, Field RL, Ye D, Hu Z, Xu K, *et al.* (2023): Induction of a torpor-like hypothermic and hypometabolic state in rodents by ultrasound. Nat Metab 5:789–803.
76. King RL, Brown JR, Newsome WT, Pauly KB (2013): Effective parameters for ultrasound-induced in vivo neurostimulation. Ultrasound Med Biol 39:312–331.
77. Gavrilov L (2016): Focused ultrasound stimulation of the peripheral nervous system: Physical basis and practical applications. Int J Mod Phys: Adv Theor Appl 1:45–118.
78. Kim H, Chiu A, Lee SD, Fischer K, Yoo SS (2014): Focused ultrasound-mediated non-invasive brain stimulation: Examination of sonication parameters. Brain Stimul 7:748–756.
79. Riis T, Kubanek J (2021): Effective ultrasonic stimulation in human peripheral nervous system. IEEE Trans Biomed Eng 69:15–22.
80. Oh SJ, Lee JM, Kim HB, Lee J, Han S, Bae JY, *et al.* (2019): Ultrasonic neuromodulation via astrocytic TRPA1. Curr Biol 29:3386–3401.e8.
81. Legon W, Strohman A (2024): Low-intensity focused ultrasound for human neuromodulation. Nat Rev Methods Primers 4:91.
82. Matt E, Radjenovic S, Mitterwallner M, Beisteiner R (2024): Current state of clinical ultrasound neuromodulation. Front Neurosci 18: 1420255.
83. Lee K, Park TY, Lee W, Kim H (2024): A review of functional neuromodulation in humans using low-intensity transcranial focused ultrasound. Biomed Eng Lett 14:407–438.
84. Sigona MK, Caskey CF (2024): Ultrasound neuromodulation: Planning and validating treatments. Curr Opin Behav Sci 59:101430.
85. Feng J, Li Z (2024): Progress in noninvasive low-intensity focused ultrasound neuromodulation. Stroke 55:2547–2557.
86. Murphy K, Fouragnan E (2024): The future of transcranial ultrasound as a precision brain interface. PLoS Biol 22:e3002884.

87. Shi Y, Wu W (2025): Advances in transcranial focused ultrasound neuromodulation for mental disorders. Prog Neuropsychopharmacol Biol Psychiatry 136:111244.
88. Attali D, Tiennot T, Schafer M, Fouragnan E, Sallet J, Caskey CF, *et al.* (2023): Three-layer model with absorption for conservative estimation of the maximum acoustic transmission coefficient through the human skull for transcranial ultrasound stimulation. Brain Stimul 16:48–55.
89. Riva-Posse P, Choi KS, Holtzheimer PE, Crowell AL, Garlow SJ, Rajendra JK, *et al.* (2018): A connectomic approach for subcallosal cingulate deep brain stimulation surgery: Prospective targeting in treatment-resistant depression. Mol Psychiatry 23:843–849.
90. Riis TS, Feldman DA, Vonesh LC, Brown JR, Solzbacher D, Kubanek J, Mickey BJ (2023): Durable effects of deep brain ultrasonic neuromodulation on major depression: A case report. J Med Case Rep 17:449.
91. Attali D, Tiennot T, Manuel TJ, Daniel M, Houdouin A, Annic P, *et al.* (2025): Deep transcranial ultrasound stimulation using personalized acoustic metamaterials improves treatment-resistant depression in humans. Brain Stimul 18:1004–1014.
92. Fan JM, Woodworth K, Murphy KR, Hinkley L, Cohen JL, Yoshimura J, *et al.* (2024): Thalamic transcranial ultrasound stimulation in treatment resistant depression. Brain Stimul 17:1001–1004.
93. Oh J, Ryu JS, Kim J, Kim S, Jeong HS, Kim KR, *et al.* (2024): Effect of low-intensity transcranial focused ultrasound stimulation in patients with major depressive disorder: A randomized, double-blind, sham-controlled clinical trial. Psychiatry Investig 21:885–896.
94. Cheung T, Li TMH, Ho YS, Kranz G, Fong KNK, Leung SF, *et al.* (2023): Effects of transcranial pulse stimulation (TPS) on adults with symptoms of depression-A pilot randomized controlled trial. Int J Environ Res Public Health 20:2333.
95. Mahdavi KD, Jordan SE, Jordan KG, Rindner ES, Haroon JM, Habelhah B, *et al.* (2023): A pilot study of low-intensity focused ultrasound for treatment-resistant generalized anxiety disorder. J Psychiatr Res 168:125–132.
96. Spivak NM, Swenson AJ, Haroon J, Holland B, Dancy M, Collins E, *et al.* (2025): Evaluating transcranial focused ultrasound stimulation (tFUS) for targeted neuromodulation in generalized anxiety disorder: A double-blind feasibility study. Brain Stimul 18:415–416.
97. Zhai Z, Ren L, Song Z, Xiang Q, Zhuo K, Zhang S, *et al.* (2023): The efficacy of low-intensity transcranial ultrasound stimulation on negative symptoms in schizophrenia: A double-blind, randomized sham-controlled study. Brain Stimul 16:790–792.
98. Badran BW, Caulfield KA, Stomberg-Firestein S, Summers PM, Dowdle LT, Savoca M, *et al.* (2022): Sonication of the anterior thalamus with MRI-guided transcranial focused ultrasound (tFUS) alters pain thresholds in healthy adults: A double-blind, sham-controlled study. Focus (Am Psychiatr Publ) 20:90–99.
99. Legon W, Strohman A, In A, Payne B (2024): Noninvasive neuromodulation of subregions of the human insula differentially affect pain processing and heart-rate variability: A within-subjects pseudo-randomized trial. Pain 165:1625–1641.
100. Hameroff S, Trakas M, Duffield C, Annabi E, Gerace MB, Boyle P, *et al.* (2013): Transcranial ultrasound (TUS) effects on mental states: A pilot study. Brain Stimul 6:409–415.
101. Riis TS, Feldman DA, Losser AJ, Okifuji A, Kubanek J (2024): Noninvasive targeted modulation of pain circuits with focused ultrasonic waves. Pain 165:2829–2839.
102. Shin DH, Son S, Kim EY (2023): Low-energy transcranial navigation-guided focused ultrasound for neuropathic pain: An exploratory study. Brain Sci 13:1433.
103. Barra A, Monti M, Thibaut A (2022): Noninvasive brain stimulation therapies to promote recovery of consciousness: Where we are and where we should go. Semin Neurol 42:348–362.
104. Monti MM, Schnakers C, Korb AS, Bystritsky A, Vespa PM (2016): Non-invasive ultrasonic thalamic stimulation in disorders of consciousness after severe brain injury: A first-in-man report. Brain Stimul 9:940–941.
105. Cain JA, Spivak NM, Coetzee JP, Crone JS, Johnson MA, Lutkenhoff ES, *et al.* (2021): Ultrasonic thalamic stimulation in chronic disorders of consciousness. Brain Stimul 14:301–303.
106. Lohse-Busch H, Reime U, Falland R (2014): Symptomatic treatment of unresponsive wakefulness syndrome with transcranially focused extracorporeal shock waves. NeuroRehabilitation 35:235–244.
107. Kohoutová L, Atlas LY, Büchel C, Buhle JT, Geuter S, Jepma M, *et al.* (2022): Individual variability in brain representations of pain. Nat Neurosci 25:749–759.
108. Yoo S, Mittelstein DR, Hurt RC, Lacroix J, Shapiro MG (2022): Focused ultrasound excites cortical neurons via mechanosensitive calcium accumulation and ion channel amplification. Nat Commun 13:493.
109. Murphy KR, Farrell JS, Bendig J, Mitra A, Luff C, Stelzer IA, *et al.* (2024): Optimized ultrasound neuromodulation for non-invasive control of behavior and physiology. Neuron 112:3252–3266.e5.
110. Vion-Bailly J, Suarez-Castellanos IM, Chapelon JY, Carpentier A, N'Djin WA (2022): Neurostimulation success rate of repetitive-pulse focused ultrasound in an in vivo giant axon model: An acoustic parametric study. Med Phys 49:682–701.
111. Lapicque L (1926): L'excitabilité en Fonction du Temps. La Chronaxie, Sa Signification et Sa Mesure. Paris, France: Presses Universitaires de France.
112. Kim HJ, Phan TT, Lee K, Kim JS, Lee SY, Lee JM, *et al.* (2024): Long-lasting forms of plasticity through patterned ultrasound-induced brainwave entrainment. Sci Adv 10:eadk3198.
113. Riis T, Feldman D, Mickey B, Kubanek J (2024): Controlled noninvasive modulation of deep brain regions in humans. Commun Eng 3:13.
114. Leung SA, Webb TD, Bitton RR, Ghanouni P, Pauly KB (2019): A rapid beam simulation framework for transcranial focused ultrasound. Sci Rep 9:1–11.
115. Pichardo S, Sin VW, Hynynen K (2010): Multi-frequency characterization of the speed of sound and attenuation coefficient for longitudinal transmission of freshly excised human skulls. Phys Med Biol 56:219–250.
116. Mueller JK, Ai L, Bansal P, Legon W (2017): Numerical evaluation of the skull for human neuromodulation with transcranial focused ultrasound. J Neural Eng 14:066012.
117. Murphy KR, Nandi T, Kop B, Osada T, Lueckel M, N'Djin WA, *et al.* (2025): A practical guide to transcranial ultrasonic stimulation from the IFCN-endorsed ITRUSST consortium. Clin Neurophysiol 171:192–226.
118. Odéen H, Payne AH, Parker DL (2025): Magnetic resonance acoustic radiation force imaging (MR-ARFI). J Magn Reson Imaging 62:20–39.
119. Mohammadjavadi M, Ash RT, Glover GH, Pauly KB (2025): Optimization of MR acoustic radiation force imaging (MR-ARFI) for human transcranial focused ultrasound. Magn Reson Med 94:1060–1071.
120. Sengupta S, Phipps MA, Chen LM, Caskey CF, Grissom WA (2025): Alternating-contrast single-shot spiral MR-ARFI with model-based displacement map reconstruction. Magn Reson Med 95:457–464.
121. Li N, Gaur P, Quah K, Butts Pauly K (2022): Improving in situ acoustic intensity estimates using MR acoustic radiation force imaging in combination with multifrequency MR elastography. Magn Reson Med 88:1673–1689.
122. Vignon F, Aubry JF, Tanter M, Margoum A, Fink M (2006): Adaptive focusing for transcranial ultrasound imaging using dual arrays. J Acoust Soc Am 120:2737–2745.
123. Webb TD, Lybbert C, Wilson MG, Odéen H, Kubanek J (2025): A physiological marker for deep brain ultrasonic neuromodulation. Neuromodulation 28:155–161.
124. Yoo SS, Bystritsky A, Lee JH, Zhang Y, Fischer K, Min BK, *et al.* (2011): Focused ultrasound modulates region-specific brain activity. Neuroimage 56:1267–1275.
125. Yang PF, Phipps MA, Newton AT, Chaplin V, Gore JC, Caskey CF, Chen LM (2018): Neuromodulation of sensory networks in monkey brain by focused ultrasound with MRI guidance and detection. Sci Rep 8:7993.

126. Chen Y, Chen Z, Estrada H, Gezginer I, Yoshihara HAI, Kindler D, *et al.* (2025): Decoding paradoxical BOLD responses to transcranial ultrasound stimulation with concurrent optoacoustic magnetic resonance imaging. Sci Adv 11:eadz1309.
127. Verhagen L, Gallea C, Folloni D, Constans C, Jensen DE, Ahnine H, *et al.* (2019): Offline impact of transcranial focused ultrasound on cortical activation in primates. Elife 8:e40541.
128. Liu D, Munoz F, Sanatkhani S, Pouliopoulos AN, Konofagou EE, Grinband J, Ferrera VP (2023): Alteration of functional connectivity in the cortex and major brain networks of non-human primates following focused ultrasound exposure in the dorsal striatum. Brain Stimul 16:1196–1204.
129. Bault N, Yaakub SN, Fouragnan E (2024): Early-phase neuroplasticity induced by offline transcranial ultrasound stimulation in primates. Curr Opin Behav Sci 56:101370.
130. Yaakub SN, White TA, Roberts J, Martin E, Verhagen L, Stagg CJ, *et al.* (2023): Transcranial focused ultrasound-mediated neurochemical and functional connectivity changes in deep cortical regions in humans. Nat Commun 14:5318.
131. Feldman D, Riis T, Kwon S, Vonesh L, Koppelmans V, Kubanek J, Mickey B (2025): Transcranial focused ultrasound neuromodulation elicits functional connectivity changes in depression. Biol Psychiatry 97:S194–S195.
132. Niu X, Yu K, He B (2022): Transcranial focused ultrasound induces sustained synaptic plasticity in rat hippocampus. Brain Stimul 15:352–359.
133. Folloni D, Verhagen L, Mars RB, Fouragnan E, Constans C, Aubry JF, *et al.* (2019): Manipulation of subcortical and deep cortical activity in the primate brain using transcranial focused ultrasound stimulation. Neuron 101:1109–1116.e5.
134. Braun V, Blackmore J, Cleveland RO, Butler CR (2020): Transcranial ultrasound stimulation in humans is associated with an auditory confound that can be effectively masked. Brain Stimul 13:1527–1534.
135. Guo H, Hamilton M, Offutt SJ, Gloeckner CD, Li T, Kim Y, *et al.* (2018): Ultrasound produces extensive brain activation via a cochlear pathway. Neuron 98:1020–1030.e4.
136. Constans C, Deffieux T, Pouget P, Tanter M, Aubry JF (2017): A 200-1380-kHz quadrifrequency focused ultrasound transducer for neurostimulation in rodents and primates: Transcranial in vitro calibration and numerical study of the influence of skull cavity. IEEE Trans Ultrason Ferroelectr Freq Control 64:717–724.
137. Sato T, Shapiro MG, Tsao DY (2018): Ultrasonic neuromodulation causes widespread cortical activation via an indirect auditory mechanism. Neuron 98:1031–1041.e5.
138. Mohammadjavadi M, Ye PP, Xia A, Brown J, Popelka G, Pauly KB (2019): Elimination of peripheral auditory pathway activation does not affect motor responses from ultrasound neuromodulation. Brain Stimul 12:901–910.
139. Riis TS, Webb TD, Kubanek J (2022): Acoustic properties across the human skull. Ultrasonics 119:106591.
140. Younan Y, Deffieux T, Larrat B, Fink M, Tanter M, Aubry JF (2013): Influence of the pressure field distribution in transcranial ultrasonic neurostimulation. Med Phys 40:082902.
141. Lee W, Kim H, Jung Y, Song IU, Chung YA, Yoo SS (2015): Image-guided transcranial focused ultrasound stimulates human primary somatosensory cortex. Sci Rep 5:8743.
142. Fomenko A, Chen KS, Nankoo JF, Saravanamuttu J, Wang Y, El-Baba M, *et al.* (2020): Systematic examination of low-intensity ultrasound parameters on human motor cortex excitability and behavior. Elife 9:e54497.
143. Legon W, Ai L, Bansal P, Mueller JK (2018): Neuromodulation with single-element transcranial focused ultrasound in human thalamus. Hum Brain Mapp 39:1995–2006.
144. Legon W, Bansal P, Tyshynsky R, Ai L, Mueller JK (2018): Transcranial focused ultrasound neuromodulation of the human primary motor cortex. Sci Rep 8:10007.
145. Ai L, Bansal P, Mueller JK, Legon W (2018): Effects of transcranial focused ultrasound on human primary motor cortex using 7T fMRI: A pilot study. BMC Neurosci 19:56.
146. Badran BW, Caulfield KA, Stomberg-Firestein S, Summers PM, Dowdle LT, Savoca M, *et al.* (2020): Sonication of the anterior thalamus with MRI-guided transcranial focused ultrasound (tFUS) alters pain thresholds in healthy adults: A double-blind, sham-controlled study. Brain Stimul 13:1805–1812.
147. Legon W, Sato TF, Opitz A, Mueller J, Barbour A, Williams A, Tyler WJ (2014): Transcranial focused ultrasound modulates the activity of primary somatosensory cortex in humans. Nat Neurosci 17:322–329.
148. Sanguinetti JL, Hameroff S, Smith EE, Sato T, Daft CMW, Tyler WJ, Allen JJB (2020): Transcranial focused ultrasound to the right prefrontal cortex improves mood and alters functional connectivity in humans. Front Hum Neurosci 14:52.